

Article

Mechanical and Thermal Properties of Polypropylene, Polyoxymethylene and Poly (Methyl Methacrylate) Modified with Adhesive Resins

Jakub Czakaj ^{1,2,3} , Daria Pakuła ² , Julia Głowacka ^{1,2} , Bogna Sztorch ² and Robert E. Przekop ^{2,*}

¹ Faculty of Chemistry, Adam Mickiewicz University in Poznań, Uniwersytetu Poznańskiego 8, 61-614 Poznań, Poland; jakub.czakaj@amu.edu.pl (J.C.); julia.glowacka@amu.edu.pl (J.G.)

² Center for Advanced Technologies, Adam Mickiewicz University in Poznań, Uniwersytetu Poznańskiego 10, 61-614 Poznań, Poland; darpak@amu.edu.pl (D.P.); bogna.sztorch@amu.edu.pl (B.S.)

³ Almara Sp. z o.o. Sp.k., 3/627 Mozarta, 02-736 Warszawa, Poland

* Correspondence: rprzekop@amu.edu.pl

Abstract: Polyoxymethylene (POM), polypropylene (PP), and poly(methyl methacrylate) (PMMA) have been blended with adhesive-grade ethylene vinyl acetate (EVA), propylene elastomer (VMX), isobutylene–isoprene rubber (IIR) and an acrylic block copolymer (MMA-nBA-MMA). The blends were prepared using a two-roll mill and injection molding. The mechanical properties of the blends, such as tensile strength, tensile modulus, elongation at maximum load, and impact resistance, were investigated. The water contact angle, melt flow rate (MFR), and differential scanning calorimetry were ascertained to evaluate the blends. The blend samples exhibited the following properties: all POM/EVA blends showed reduced crystallinity compared to neat POM; the 80% PMMA/20% MMA-nBA-MMA blend showed improved impact resistance by 243% compared to the neat PMMA. An antiplasticization effect was observed for POM/EVA 1% blends and PMMA/EVA 1% blends, with MFR reduced by 1% and 3%, respectively. The MFR of the PP/IIR 1% blend increased by 5%, then decreased below the MFR near the polymer for the remaining IIR concentrations.

Keywords: PMMA; PP; POM; elastomer; blend; mechanical properties; thermal properties



Citation: Czakaj, J.; Pakuła, D.; Głowacka, J.; Sztorch, B.; Przekop, R.E. Mechanical and Thermal Properties of Polypropylene, Polyoxymethylene and Poly (Methyl Methacrylate) Modified with Adhesive Resins. *J. Compos. Sci.* **2024**, *8*, 384. <https://doi.org/10.3390/jcs8100384>

Academic Editor: Ignazio Blanco

Received: 9 August 2024

Revised: 12 September 2024

Accepted: 19 September 2024

Published: 24 September 2024



Copyright: © 2024 by the authors. Licensee MDPI, Basel, Switzerland. This article is an open access article distributed under the terms and conditions of the Creative Commons Attribution (CC BY) license (<https://creativecommons.org/licenses/by/4.0/>).

1. Introduction

1.1. Enhancing POM with Elastomers

POM is a high-performance engineering thermoplastic widely recognized for its superior mechanical properties, which include high strength, stiffness, excellent dimensional stability, and resistance to wear and abrasion [1–4]. These attributes, along with its low friction and good chemical resistance, make POM an ideal material for a wide range of applications, particularly in injection molding processes. The ability of POM to melt uniformly and flow well into molds facilitates the production of high-volume, intricate parts with tight tolerances [5]. As a result, injection-molded POM parts are commonly found in automotive powertrains, appliances, medical devices, industrial equipment, and more. Typical components include gears, rollers, bushings, sprockets, cams, fasteners, nozzles, and shaft couplings [6]. Despite its advantageous properties, POM has some shortcomings, such as low-notch sensitivity, poor heat resistance, and prohibitive costs, which limit its application scope [7]. Consequently, modifying POM resin to expand its applications and improve its processing technology has been a significant research focus in recent years [8]. Various elastomers, including polyolefin elastomer (POE) [9], thermoplastic polyurethane (TPU) [2,10,11], ethylene propylene diene terpolymer (EPDM) [12], and acrylics [13,14], have been studied for their effects on POM blends. Modifying POM with elastomers such as EVA presents both opportunities and challenges. EVA, with its low-glass transition temperature, can effectively absorb impact energy, making it a suitable impact modifier for

POM, especially at low temperatures [12]. The modification of POM with EVA has been found to influence parameters such as the melt flow index, tensile tests, surface resistance, contact angle, as well as thermal properties of the resulting blend [8]. EVA may also serve as a copolymer compatibilizer in POM blends [12,15–17]. The introduction of EVA or EBA into POM/EPDM blends has notably enhanced impact resistance [12,18]. However, achieving the significant toughening of POM at room temperature requires well-dispersed elastomer particles with a critical interparticle distance. Additionally, good compatibility and interfacial adhesion between POM and the elastomeric modifier are crucial for effective toughening [19]. While modifying POM with elastomers like EVA can improve impact toughness, challenges such as reduced strength and rigidity, poor antistatic performance, and limitations in solvent and high-temperature resistance must be addressed. Research on elastomer-modified POM blends highlights the potential for enhancing the mechanical properties of POM through elastomer incorporation. By carefully selecting elastomers, optimizing blend compositions, and refining processing conditions, it is possible to improve the toughness, impact resistance, and low-temperature performance of POM blends.

1.2. Enhancing PP with Elastomers

PP is a versatile thermoplastic polymer known for its exceptional mechanical properties, chemical resistance, and ease of processing [20–25]. PP exhibits high tensile strength and modulus, making it suitable for applications that require good load-bearing capacity and dimensional stability. The polymer's semi-crystalline structure, resulting from the regular arrangement of methyl groups along the backbone, contributes to its excellent stiffness and rigidity.

Isotactic polypropylene (iPP) is a semi-crystalline thermoplastic polymer with a regular structure where all the methyl groups are oriented on the same side of the polymer backbone. This stereoregular arrangement allows iPP to crystallize, resulting in high mechanical strength and chemical resistance [26–28]. The properties of iPP can be tailored by controlling the molecular weight, molecular weight distribution, nature of the crystal phase, and atactic content during polymerization [29,30].

It finds applications in consumer goods, industrial products [31], the automobile industry [25,32], and furniture manufacturing [33]. Used for interior trims, bumpers [34], and under-the-hood components due to its adequate impact resistance in ambient temperatures, heat resistance, and cost-effectiveness [35], PP fibers find use in concrete reinforcement [36]. Despite its numerous benefits, the application of PP is constrained by its limited fracture toughness, especially at low temperatures [37–41]. The impact resistance of PP is commonly improved using blending or dynamic vulcanization with elastomers like EPDM [42,43], ethylene-octene elastomers [44], EVA [45], or propylene-based elastomers [46,47]. Thermoplastic vulcanizate (TPV) PP/EPDMs are commonly used in the automotive industry. Both their strength and elasticity may be improved by introducing nucleating agents [48]. Vistamaxx polymers, primarily composed of isotactic propylene repeat units with a random ethylene distribution, are notable for their compatibility and performance enhancements in various applications with high filler loading [37,49,50]. The presence of isotactic propylene segments allows Vistamaxx polymers to be highly compatible with other polyolefins, such as PP and polyethylene (PE). This enables the creation of blends with improved properties, as demonstrated using Vistamaxx as an impact modifier in high-flow thermoplastic polyolefin (TPO) compounds based on homopolypropylene and impact copolymers [46,51,52].

1.3. Enhancing PMMA with Elastomers

PMMA is widely recognized for its versatility across various sectors, including automotive, construction, lighting, and biomedical applications, due to its outstanding properties, such as high strength, stiffness, and biocompatibility. PMMA is favored for automotive components due to its transparency, excellent injection molding properties, chemical resistance, superior weatherability, favorable acoustic qualities, robust mechanical properties, and cost-effectiveness [53–55]. Its high light transmittance and resistance to UV light and

chemicals are beneficial for creating functional surfaces and optical devices [56–58]. However, PMMA is known to be brittle at room temperature, with a low elongation at break (~5%), which limits its applications.

Efforts to enhance the toughness of PMMA often involve melt blending with various types of rubber, including natural rubber, TPU, an EVA copolymer or a core–shell approach involving compatibilizers [59–63]. This process aims to improve the material's resilience without significantly compromising its inherent properties and can substantially increase its toughness, with notable improvements on impact resistance. Acrylic triblock copolymers (i.e., Nanostrength®—Arkema, Colombes, France and Kurarity™—Kurashiki, Okayama, Japan), consisting of PMMA hard-blocks and poly(*n*-butyl acrylate), or poly(*n*-butyl acrylate/2-ethylhexyl acrylate) soft-blocks, are an alternative to PMMA for applications requiring high toughness and optical transparency [64–66]. They share many similarities to styrenic block copolymers as the toughness of acrylic triblock copolymers is determined by the soft-block concentration [64]. Nevertheless, mechanical properties, particularly the strength and stiffness, of resilient acrylic triblock copolymers exhibit considerably lower values in comparison to commercially available PMMA grades, especially rubber-toughened PMMAs. KURARAY has succeeded in designing the perfect living polymerization of *n*BA using a Lewis base combined with di-phenoxyalkyl aluminum (LA system) [67–69]. “Kurarity™” acrylic block copolymers, synthesized using the LA system, are pure PMMA-*b*-PnBA-*b*-PMMA triblock (MnBM) copolymers consisting of the sequential polymerization of MMA, *n*BA, and MMA [68].

The polymer blocks of Kurarity™, namely PMMA and PnBA, exhibit the compatibility or miscibility with traditional polar polymer materials. When employed as an additive in rigid materials, Kurarity™ fulfills various functional roles, including serving as an impact modifier, softening agent, fluidity enhancer, and adhesion enhancer. Kurarity™ finds application in PMMA, polybutylene terephthalate (PBT), polylactic acid (PLA), and polyvinyl chloride (PVC). In instances where the composite material comprises soft or elastomeric substances such as the styrenic thermoplastic elastomer, TPU, or soft PVC, the incorporation of “KURARITY™” can lead to enhancements in paintability and the adhesion properties of the material [68].

The aim of this work was to develop and evaluate the effects of blending adhesive-grade resins with commercial polymers, specifically POM, PP, and PMMA, to enhance their mechanical properties for injection molding applications. This research focuses on evaluating the effects of these blends on tensile strength and impact resistance, thermal and surface properties, blend miscibility, and melt flow rate. By integrating adhesive resins, the goal is to improve the toughness, processability, and overall performance of these polymers, thereby broadening their potential industrial uses. Although the toughening effects of elastomers on thermoplastic resins are known, the effects of adhesive resins on the properties of engineering thermoplastics used in the current study has not been investigated before.

2. Materials and Methods

2.1. Materials

The PP, specifically the Moplen HP648T grade (melt flow rate 53 g/10 min (230 °C/2.16 kg), density 0.90 g/cm³ (23 °C)), was acquired from Basell Orlen Polyolefins (Poland). The IIR, specifically the BK-1675N grade (Mooney viscosity 47–57 MU ML 1 + 8 (125 °C), density 0.92 g/cm³), was acquired from Konimpex (Poland). The propylene elastomer (VMX), specifically the Vistamaxx 8880 grade (viscosity 1200 mPas at 190 °C, density 0.88 g/cm³), was acquired from Biesterfeld (Poland). The PMMA, specifically the Altuglas VML100 grade (melt flow rate 14.5 g/10 min (230 °C/3.8 kg), density 1.18 g/cm³), was acquired from Trinseo PLC (Berwyn, PA, USA). Poly(methyl methacrylate-*n*-butyl acrylate-*n*-butyl methacrylate) (MMA-*n*BA-MMA), specifically Kurarity LA3320 (MFR 31 g/10 min (190 °C/2.16 kg)) was acquired from Mitsui (Skarbimierz, Poland). EVA, specifically Repsol P40055 (MFR 55 g/10 min (190 °C/2.16 kg)), was acquired from Torimex (Konstan-

tynów Łódzki, Poland). POM, specifically Tarnoform 300 grade (melt flow rate 9.0 g/10 min (190 °C/2.16 kg); density 1.41 g/cm³), was acquired from Azoty Tarnow™ (Tarnów, Poland).

2.2. Methods

2.2.1. Blend Preparation

The blends were prepared using a laboratory two-roll mill ZAMAK MERCATOR WG 150/280. Prior to blending, the base polymer and the modifier were dried at 55 °C/24 h. A portion of 800 g of the base polymer was heated until melting, and then the secondary polymer was added until a binary blend was obtained with a concentration of 20% by weight (based on the weight of the entire system). The temperature of the rolls was set to 220 °C for PMMA, 210 °C for POM, and 200 °C for PP blends. The roll mill speed was set to 15 rpm. The nip was set to 0.5 mm initially and then increased gradually to 3 mm as the material was added. The blends were mixed for 15 min, including rolling with a spatula and passing the rolls endwise at least 5 times. The resulting blend was then shredded using a SHINI SG-1417-CE mill. Both the blend and neat polymer were dried at 55 °C/24 h before injection molding. The obtained blend was reground with a concentration of 20% by weight and was diluted with neat base polymer granules to the final concentrations of 1.0, 2.5, 5, 10, and 20% by weight, respectively. The granule–regrind mix was mechanically agitated to ensure even distribution. Both the regrind and neat polymer granules exhibited similar size to ensure there was no separation in the hopper after mixing. Standardized specimen type 1A and type B for mechanical tests were obtained according to ISO 20753:2019-01 [70]. The samples type A1 were injected using an Engel e-victory 170/80 injection molder machine. The temperature profiles were 215 °C, 225 °C, 225 °C, 205 °C, and 40 °C on the nozzle, front, center, rear, and feed zone, respectively. The pressure profile was set to 850 bar at 0 s, 1000 bar at 6 s, and 200 bar at 8 s. The injection volume was 32.5 cm³, and the total cycle time was 50 s. Type B specimens for impact tests with dimensions of 80 × 10 × 4 mm (length × width × thickness) were obtained by mechanical shaping from the middle section of injected samples of type A1.

2.2.2. Water Contact Angle Measurement

The water contact angle (WCA) was performed using the sessile drop technique under standard ambient temperature and pressure conditions, using a Krüss DSA100 goniometer (Krüss, Hamburg, Germany) in accordance with the ISO 19403-2:2017 [71]. Each sample underwent three distinct measurements, employing a 5 µL water droplet for each measurement, and subsequently, the outcomes were averaged to reduce the influence of surface irregularities.

2.2.3. Melt Flow Rate Measurement

The effect of the modifier addition on the mass flow rate (MFR) was also determined. Measurements were conducted with a Haida plastometer (RD824 model), according to the ISO 1133 standard [72]. For PP and POM, the temperature was maintained at 190 ± 0.5 °C, while for PMMA, the temperature was 230 ± 0.5 °C, and the piston load applied was 2.16 kg. The sample was cut using an automatic cutter; for MFR determination, 5–10 cuts were used, and imperfect extrudates were discarded.

2.2.4. Mechanical Properties Measurement

The samples for tensile tests were injected into type 1B dumbbell specimens according to ISO 527-1:2019 [73], respectively. Tests of the obtained specimens were performed on a universal testing machine INSTRON 5969 with a maximum load force of 50 kN. The testing machine was not equipped with an extensometer. The traverse speed for tensile measurements was set at 2 mm/min. The Charpy impact test was conducted in accordance with the ISO 179-1 standard [74] (samples without notches). The tests were performed using an Instron Ceast 9050 instrument equipped with a pendulum hammer with a maximum

energy of 25 J. Seven measurements were made for each tested material, with the two most extreme values excluded.

2.2.5. Differential Scanning Calorimetry

Differential scanning calorimetry (DSC) analysis was conducted employing a NET-ZSCH204 F1 Phoenix calorimeter (Selb, Germany). Samples weighing 5 ± 0.2 mg were loaded into aluminum crucibles with punctured lids. The experiments were conducted under a nitrogen atmosphere within a temperature range of -60 °C– 220 °C and at a heating and cooling rate of 10 °C/min in accordance with the ISO 11357-1:2023 standard [75]. DSC was conducted on reference samples and blends with a 10% concentration to identify characteristic phase transitions and changes occurring in the samples.

3. Results and Discussions

3.1. Rheology

The melt volume flow rate (MVR) or melt flow rate (MFR) is an important characteristic of the flow properties of polymeric materials. It is an assessment of the average molecular mass and is an inverse measure of melt viscosity; in other words, the higher the MFR, the more the polymer flows under test conditions [76]. The MVR test is a quick and convenient way of analyzing the effect of additives and fillers on the flow of modified materials as well as batch-to-batch flow variations. This simple analysis is widely used in the industry as a quality control test.

All additives, except for IIR, exhibited a higher MFR than the corresponding modified resin. As seen in Figures 1–3, the obtained results correspond to the expectation that the MFR of the resulting blends should be an intermediate between the base and the modifying resin [77,78]. Contrary to expectations, PMMA and POM blended with EVA exhibited anti-plasticization effects at concentrations of 1–2.5%, as depicted in Figure 1.

Generally, as the temperature increases, the macromolecular polymer chains exhibit higher mobility. This leads to decreased melt viscosity and increased MFR [15]. IIR exhibits higher viscosity than PP and may not be easily dispersed using low-shear equipment. Therefore, the droplets of the rubbery phase may have formed a coarse morphology affecting the flow. It is a known phenomenon that in rubber/PP blends, the morphology is governed by breakup/coalescence during mixing [79,80].

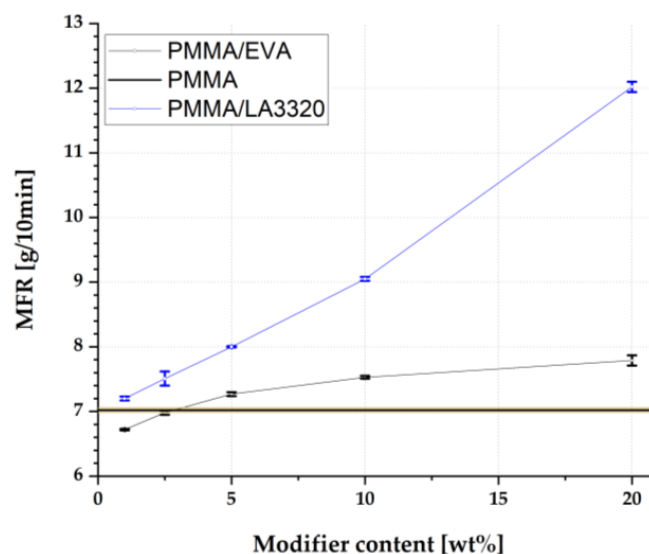


Figure 1. Results of MFR measurement of PMMA blended with EVA and Kurarity LA3320.

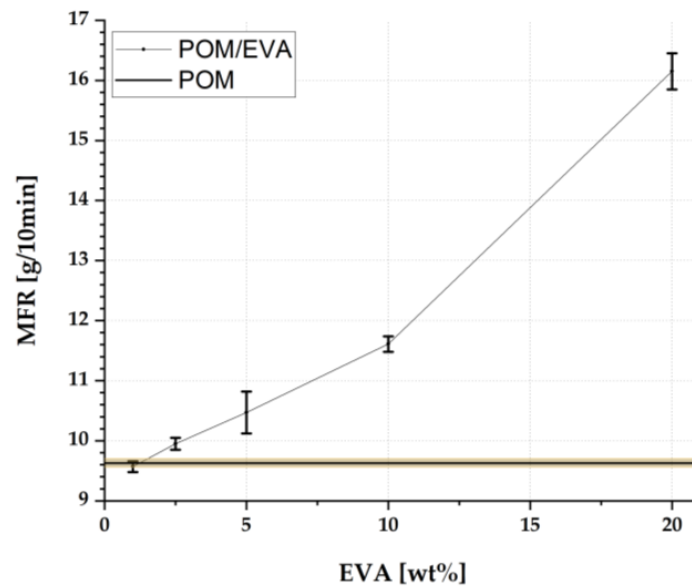


Figure 2. Results of MFR measurement of POM blended with EVA.

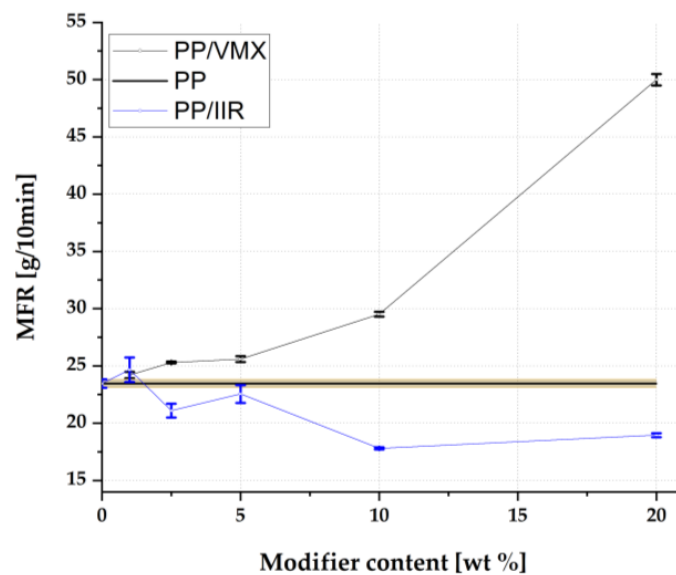


Figure 3. Results of MFR measurement of PP blended with VMX and IIR.

3.2. Mechanical Analysis

In the context of designing new engineering materials, determining fundamental strength parameters such as impact resistance and tensile strength is crucial. The mechanical properties of neat polymers differ significantly from those of the blends and composites made with them. In this study, a series of mechanical tests were conducted on POM, PMMA, and PP polymer samples with various additives, including EVA elastomer, MMA-nBA-MMA copolymer, IIR, and VMX. Introducing an elastomeric component with high ductility and plasticizing characteristics into the presented polymer matrices resulted in a decrease in tensile strength as the mass proportion of the additive increased. The tensile and Charpy impact test results are shown in Table 1.

Table 1. Mechanical properties summary table.

Sample Name	Concentration (%)	R _m (MPa)	E (MPa)	ε (%)	K _{IC} (kJ/m ²)
POM/EVA	0.0	59.00 ± 0.48	1819 ± 36	10.46 ± 0.15	314.13 ± 14.66
	1.0	58.27 ± 0.17	1862 ± 43	9.91 ± 0.17	348.00 ± 15.07
	2.5	55.96 ± 0.79	1871 ± 27	9.67 ± 0.23	322.39 ± 7.50
	5.0	52.36 ± 1.19	1721 ± 59	9.67 ± 0.13	311.72 ± 11.25
	10.0	45.93 ± 1.03	1611 ± 46	9.84 ± 0.19	260.40 ± 15.31
	20.0	35.28 ± 0.34	1288 ± 17	10.25 ± 0.10	175.38 ± 12.39
PMMA/EVA	0.0	66.05 ± 1.46	2922 ± 38	3.55 ± 0.25	20.35 ± 0.71
	1.0	65.78 ± 1.61	3172 ± 39	2.87 ± 0.14	18.40 ± 0.92
	2.5	60.92 ± 2.81	3031 ± 59	2.73 ± 0.23	18.50 ± 1.11
	5.0	61.22 ± 1.72	2843 ± 60	3.29 ± 0.35	19.38 ± 0.38
	10.0	54.26 ± 2.56	2492 ± 58	3.33 ± 0.51	22.16 ± 1.66
	20.0	43.79 ± 0.71	1897 ± 28	4.19 ± 0.23	26.64 ± 4.82
PMMA/MMA-nBA-MMA	1.0	63.74 ± 0.70	2909 ± 30	3.38 ± 0.10	21.31 ± 0.70
	2.5	61.37 ± 4.16	2808 ± 28	3.43 ± 0.43	22.04 ± 0.96
	5.0	60.30 ± 1.46	2729 ± 50	3.30 ± 0.55	22.23 ± 1.11
	10.0	59.38 ± 1.83	2688 ± 60	3.68 ± 0.31	22.27 ± 1.53
	20.0	32.49 ± 5.70	1424 ± 272	5.77 ± 1.19	49.49 ± 7.64
PP/IIR	0.0	34.21 ± 0.60	1324 ± 14	8.63 ± 0.16	93.96 ± 4.23
	1.0	33.34 ± 0.72	1301 ± 37	8.09 ± 0.18	53.52 ± 2.85
	2.5	32.11 ± 0.94	1273 ± 51	7.68 ± 0.19	42.95 ± 7.03
	5.0	32.04 ± 0.80	1271 ± 56	8.15 ± 0.25	54.27 ± 8.16
	10.0	26.37 ± 0.57	1257 ± 35	6.84 ± 0.15	39.04 ± 2.10
	20.0	28.62 ± 4.36	1204 ± 97	7.13 ± 0.59	45.56 ± 6.14
PP/VMX	1.0	34.00 ± 0.28	1331 ± 26	8.70 ± 0.18	100.82 ± 15.71
	2.5	33.87 ± 0.66	1280 ± 48	8.83 ± 0.26	119.53 ± 3.59
	5.0	32.84 ± 0.55	1206 ± 23	9.33 ± 0.25	15.62 ± 3.27
	10.0	30.08 ± 0.76	1068 ± 37	9.71 ± 0.32	17.72 ± 4.87
	20.0	27.23 ± 1.99	1099 ± 23	6.15 ± 0.73	38.28 ± 9.70

The results indicate that both tensile strength (R_m) and Young’s modulus (E) generally decrease as the concentration of the secondary component increases across all polymer blends. Elongation at break (ε), while showing minor fluctuations, tends to either decrease or stabilize with higher concentrations of the secondary component. For fracture toughness (K_{IC}), the PMMA/EVA and PMMA/MMA-nBA-MMA blends exhibit an increase in impact resistance at specific concentrations (Figure 4), whereas the POM/EVA, PP/IIR, and PP/VMX blends display a general decrease. These findings suggest that the mechanical properties of the polymer blends are significantly influenced by the concentration of their components and their miscibility, affecting their suitability for different applications based on the desired mechanical performance.

In both POM/EVA blends, the tensile strength and impact resistance exhibit a linear decrease with the increasing elastomer content (Figures 5 and 6). This is attributed to the decrease in the degree of crystallinity with the increasing content of the elastomer, as shown by thermal analysis. Related results showing a decrease in mechanical properties were reported by Galeja et al. and Uthaman et al. [8,12].

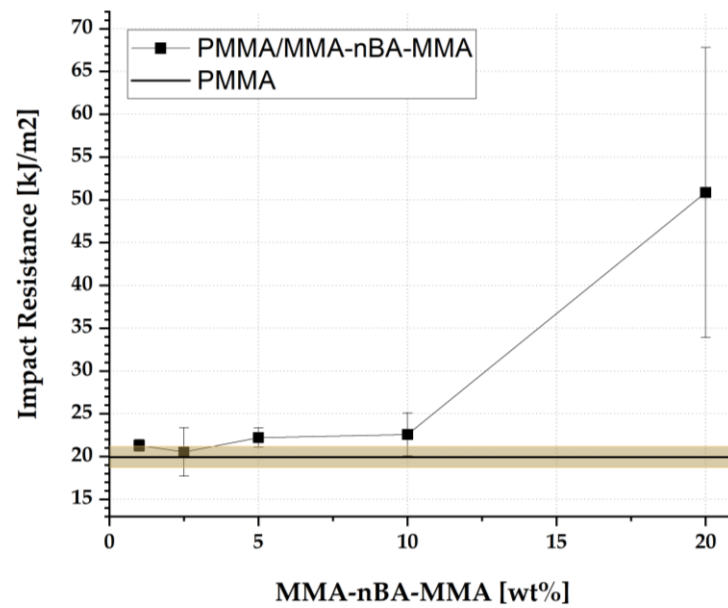


Figure 4. Results of impact resistance measurement of PMMA blended with MMA-nBA-MMA.

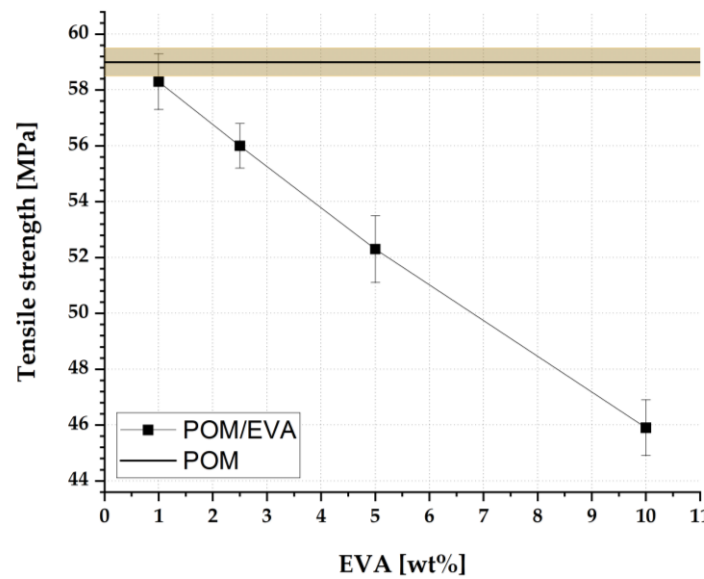


Figure 5. Results of tensile strength of POM blended with EVA.

The tensile strength of PMMA/EVA decreases gradually from 63.74 to 32.49 MPa with the increasing EVA content. The addition of the elastomer is expected to reduce the maximum load and stiffness of the blends. Surprisingly, the impact resistance decreased at EVA loadings <5% but was higher than the reference at higher loadings. The general trend is consistent with the results of similar blends of PMMA/EVA (29% VA) obtained by Poomalai et al. [81]. However, in this study, EVA (40% VA) reduces impact resistance at low concentrations.

The blend of the MMA-nBA-MMA block copolymer with PMMA exhibited an impact resistance of 49.49 kJ/m² at a 20% concentration, which is a 243% improvement compared to the neat resin's value of 20.35 kJ/m². However, the blend gradually lost transparency with the addition of the block copolymer. Similar effects have been observed in PS/SEBS miscible blends [82]. The impact resistance of PS was improved to be over 2-fold at a 13% SEBS concentration. The dissipation of energy during impact testing by the soft block was

possible due to the miscibility between the hard block of the block copolymer and the main component of the blend.

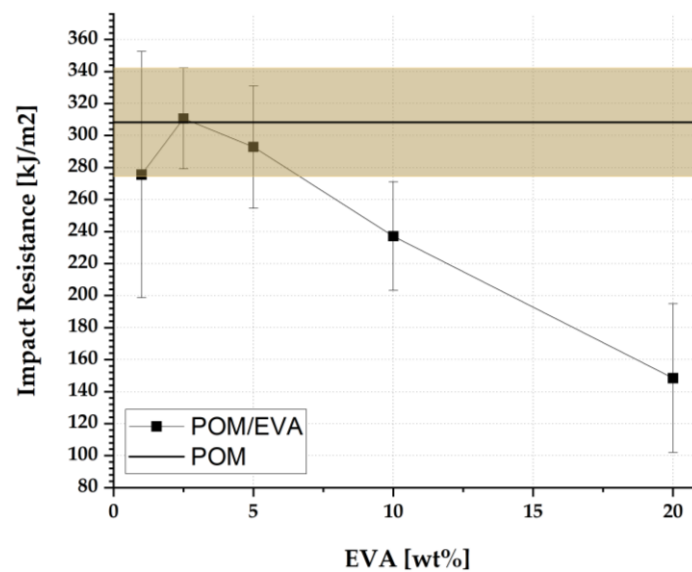


Figure 6. Results of impact resistance measurement of POM blended with EVA.

The tensile strength of PP blends decreases with the addition of both IIR and VMX. The possible immiscibility between polymers, as well as the difference between elastic moduli, causes the dispersed rubber particles to act as a filler, which does not transfer the mechanical force effectively. The impact resistance was expected to increase [83]; however, due to big viscosity mismatch between both phases and an insufficient shear during mixing phase, a coarse blend might have resulted in obtaining inferior impact resistance. The addition of 2.5% of VMX improved the impact resistance from 93.96 to 119.53 kJ/m²; however, a higher concentration resulted in a brittle material with low impact resistance. In contrast to the improved results obtained with the elastomeric VMX grades obtained by Yang et al. [47], the adhesive grade VMX showed a decrease in impact resistance.

In all investigated blends, apart from PMMA/MMA-nBA-MMA blends, the reduced mechanical properties are caused by the poor miscibility of the blend components, which results in a poor interphase adhesion and force transfer between phases. The elastomeric component effectively acts as a filler, and due to smaller elastic moduli compared to the plastomer phase, the dispersed elastomer may be effectively treated as a void in the plastomer matrix. In the case of PMMA/MMA-nBA-MMA blends, good miscibility between MMA blocks and the PMMA phase was expected. This was evidenced by an increase in impact resistance. Due to appropriate miscibility, the impact energy may be efficiently distributed and dissipated in the nBA blocks, increasing the impact resistance of the blends.

3.3. Water Contact Angle

Water contact angle analysis was conducted to evaluate the surface properties of both the base polymers and their blends and to investigate the effect of varying component ratios on these properties. Modifying hydrophilic/hydrophobic properties is crucial to the design of new materials with desirable surface properties, especially in the context of applications where moisture resistance is important, such as in the packaging and chemical industries. The results of water contact angle measurements are shown in Table 2. The base polymers, i.e., POM, PMMA, and PP, exhibited a water contact angle of less than 90°, indicating their hydrophilic nature. However, a WCA value of 88.3° for PP is close to hydrophobic properties. Incorporating EVA into both POM and PMMA resulted in a reduction in the WCA, indicating a shift towards more hydrophilic properties in these

blends. This effect is particularly pronounced in the POM/EVA blends. The water contact angle decreased as the EVA content in the materials increased, which is likely related to the presence of polar vinyl acetate (VA) groups in the EVA structure [84]. The introduction of MMA-nBA-MMA into PMMA had a minor impact on increasing the contact angle of the materials. The slight change in the contact angle may be attributed to similarities in their chemical structures and the good compatibility between them. For PP/IIR blends, goniometric analysis revealed that the water contact angle remained relatively constant at lower concentrations (0–5%), ranging between 87.9° and 88.3°. This suggests that the surface structure of the material did not undergo significant changes within these concentration ranges, thereby maintaining consistent surface properties. However, at higher concentrations (10% and 20%), a notable decrease in the water contact angle to 81.4° and 80.2° was observed, which may be attributed to changes in the blend. PP/VMX blends demonstrated higher hydrophobicity compared to the base PP. The water contact angle values for these blends exceeded 90°, indicating a shift towards more hydrophobic properties. The increase in the contact angle ranged from 1.9° to 4.4° over the base sample, underscoring the impact of VMX on the surface characteristics of the blends. The incorporation of Vistamaxx into polypropylene, which contains nonpolar isotactic propylene repeat units with randomly distributed ethylene segments, preserved or enhanced the overall hydrophobicity of the material. The analysis of contact angles, thus, provides crucial insights into the surface behavior of polymer blends, guiding the design of materials with targeted properties for various industrial applications. By adjusting the component ratios, it is possible to fine-tune the balance between hydrophilicity and hydrophobicity, thereby optimizing the performance of the resulting materials for specific functional requirements.

Table 2. Results of water contact angle analysis.

Sample Name/Concentration [%]	Water Contact Angle [°]					
	0	1	2.5	5	10	20
POM/EVA	79.0 ± 1.0	78.5 ± 1.0	76.1 ± 1.5	77.5 ± 3.0	68.4 ± 2.0	69.8 ± 3.5
PMMA/EVA	78.3 ± 1.0	71.6 ± 3.0	72.6 ± 2.0	75.2 ± 1.5	73.6 ± 1.0	75.1 ± 2.0
PMMA/MMA-nBA-MMA	78.3 ± 1.0	78.5 ± 2.0	79.3 ± 1.0	81.4 ± 3.0	80.0 ± 1.5	80.7 ± 2.0
PP/IIR	88.3 ± 0.5	88.3 ± 1.0	87.9 ± 0.5	88.0 ± 1.0	81.4 ± 3.0	80.2 ± 2.0
PP/VMX	88.3 ± 0.5	91.7 ± 1.0	90.2 ± 1.0	92.7 ± 2.0	92.1 ± 0.5	92.3 ± 1.5

3.4. Differential Scanning Calorimetry (DSC)

The melting temperature (T_m), crystallization temperature (T_c), and glass transition temperature (T_g) were determined from the second measurement cycle using DSC (Table 3).

Table 3. Thermal properties based on DSC analysis.

Sample	T_g [°C]	T_c [°C]	T_m [°C]	Degree of Crystallinity [%]
PP	-	123.1	164.0	35.8
PP/IIR	-	122.9	163.7	38.5
PP/VMX	-	122.2	163.8	35.9
POM	-	144.9	168.2	42.3
POM/EVA	-	144.8	167.0	33.4
PMMA	100.6	-	-	-
PMMA/EVA	100.2	-	-	-
PMMA/MMA-nBA-MMA	101.3	-	-	-

For PP and its blends (Figure 7), an endothermic peak was observed from which the melting temperature $T_{mPP} = 164.0$ °C and the crystallization peak $T_{cPP} = 123.1$ °C were determined. In the case of the blends, no significant changes were noted ($T_{mPP/VMX} = 163.8$ °C,

$T_{mPP/IIR} = 163.7\text{ }^{\circ}\text{C}$, $T_{cPP/VMX} = 122.2\text{ }^{\circ}\text{C}$, $T_{cPP/IIR} = 122.9\text{ }^{\circ}\text{C}$). Additionally, the glass transition temperature (T_g), expected to occur below $-20\text{ }^{\circ}\text{C}$, was not observed in the blends, which might be due to the insufficient concentration of VMX or IIR in the samples. The crystallinity of the composites was determined based on DSC curves (Table 3). Both for the reference polymer and blends, the level of crystallinity was similar and ranged from 35% to 39%. The crystalline phase fraction was calculated using Equation (1).

$$X_c = \frac{\Delta H_m}{\Delta H_m^0 \times \omega_i} \times 100\% \tag{1}$$

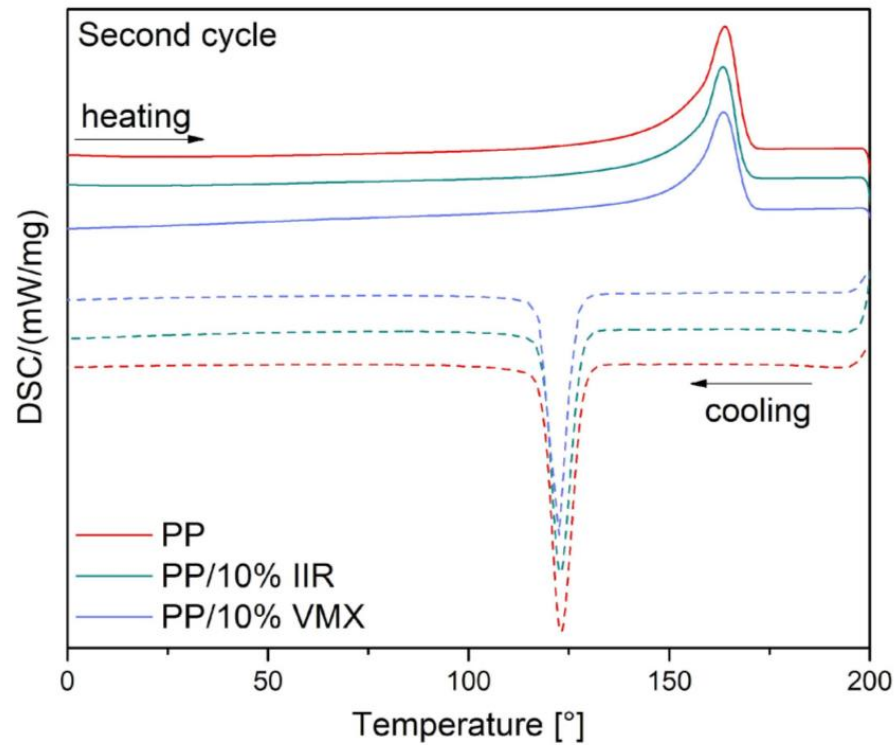


Figure 7. DSC curves for PP and blends.

X_c —degree of crystallinity, ΔH_m = enthalpy of melting of the tested material; ΔH_m^0 = enthalpy of melting of a completely crystalline substance, assuming PP—209 J/g [85]; and ω_i = weight fraction of polymer.

Based on the DSC curves, characteristic phase transitions were determined for POM, including the melting temperature (T_m) and crystallization temperature (T_c) (Figure 8). For the unmodified polymer, phase transitions occurred at temperatures of $168.2\text{ }^{\circ}\text{C}$ (T_m) and $144.9\text{ }^{\circ}\text{C}$ (T_c), respectively. Similar to PP-based blends, no significant changes in temperatures were observed for POM/EVA ($T_m = 167.0\text{ }^{\circ}\text{C}$; $T_c = 144.8\text{ }^{\circ}\text{C}$). The crystallinity was calculated according to Equation (1), assuming that for a neat polymer (100% crystalline), the enthalpy of melting would be 326 J/g [86]. The determined crystallinity of the unmodified polymer was found to be 42.3%, whereas the addition of an elastomer (EVA) resulted in a decrease in the degree of crystallinity by 8.9 (Table 3). This indicates that the presence of EVA has a notable impact on the crystalline structure of the polymer blend, leading to a reduction in its overall crystallinity.

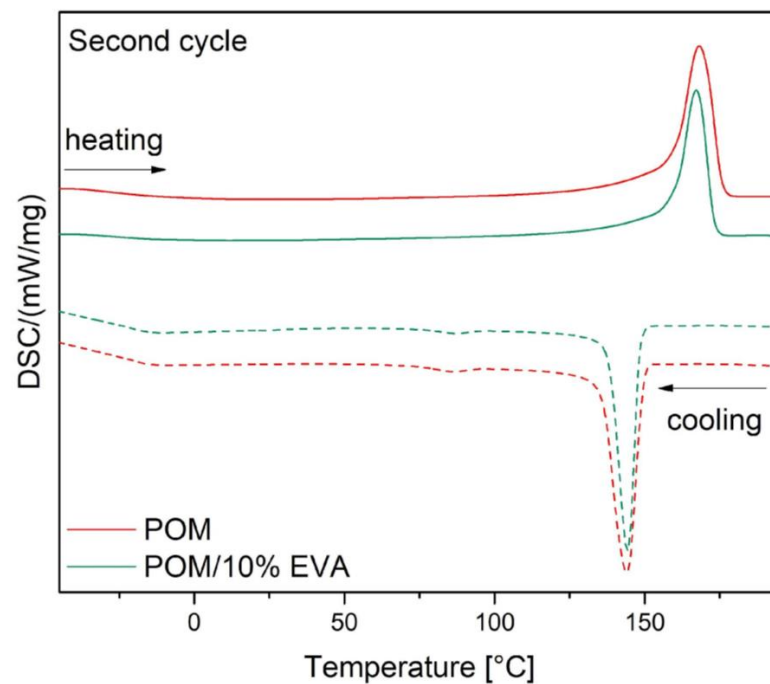


Figure 8. DSC curves for POM and blends.

The DSC curves of poly(methyl methacrylate) (PMMA) and its blends (Figure 9) indicate the presence of a single endothermic peak corresponding to the glass transition temperature (T_g). For unmodified PMMA, the T_g is 100.6 °C, while for the PMMA/EVA and PMMA/MMA-nBA-MMA blends, the T_g values are 100.2 °C and 101.3 °C, respectively. It was observed that the T_g for each system was similar, indicating good miscibility between the base polymer and additives. This suggests that the introduction of additives did not significantly affect the glass transition temperature, implying thermal stability in the investigated systems.

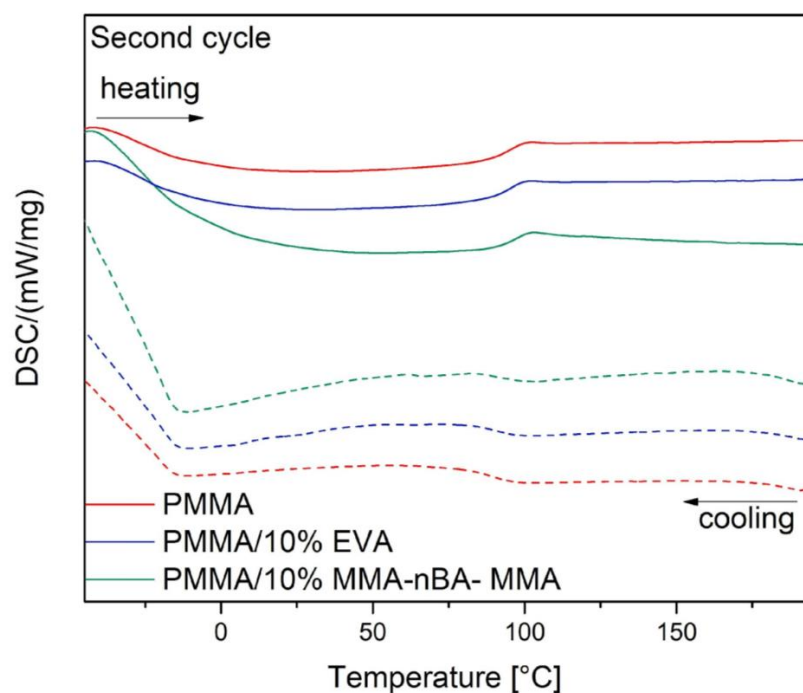


Figure 9. DSC curves for PMMA and blends.

4. Conclusions

Engineering thermoplastics were blended with adhesive-grade elastomers to improve their toughness without compromising their inherent desirable properties. In the case of POM/EVA blends, an increase in the elastomer content resulted in a decrease in both tensile strength and modulus, which was attributed to a reduction in crystallinity. Despite these reductions in strength and rigidity, the toughness of the material improved significantly, demonstrating a beneficial trade-off. An addition of 10–20 wt % of EVA may be added to POM to improve its impact resistance at the cost of reduced tensile strength. For PMMA blends, the impact resistance may be improved by 243% compared to neat resin by adding 20% of P(MMA-*n*Ba-MMA); however, the transparency of the blends will be reduced, which is consistent with the results reported in [64]. In the case of PP blends, the tensile strength decreased, though the impact resistance was initially improved by the addition of VMX.

The melting and crystallization temperatures of the base polymers did not change with the addition of elastomers; however, a decrease in crystallinity was observed in the POM blends. The blends of PMMA showed good miscibility between the base polymer and the modifying resins.

The hydrophobicity of PP/VMX blends was increased compared to the neat PP, making them more resistant to moisture; however, any addition of VMX decreased the mechanical properties of PP. Conversely, POM/EVA and PMMA/EVA blends became more hydrophilic, enhancing their ability to interact with moisture. This shift in hydrophilic and hydrophobic properties can be advantageous depending on the specific application requirements, such as in moisture-sensitive environments. The melt flow rate (MFR) of the blends generally increased with the addition of modifying resins, which suggests an improvement in processability. However, the addition of EVA led to anti-plasticizing effects at lower concentrations, where the material exhibited reduced flowability despite the presence of an elastomeric additive. This underscores the importance of carefully controlling the concentration of additives to achieve the desired balance between flow characteristics and mechanical properties.

Author Contributions: Conceptualization, J.C., B.S. and R.E.P.; methodology, R.E.P. and J.C.; validation, J.C., D.P., J.G. and B.S.; formal analysis, J.C., D.P. and J.G.; investigation, J.C., D.P. and J.G.; resources, J.C., B.S. and R.E.P.; data curation, J.C., D.P. and J.G.; writing—original draft preparation, J.C., D.P. and J.G.; writing—review and editing, B.S. and R.E.P.; visualization, J.C., D.P. and J.G.; supervision, B.S. and R.E.P.; project administration, R.E.P.; funding acquisition, R.E.P. All authors have read and agreed to the published version of the manuscript.

Funding: This research was funded by the Ministry of Education and Science: implementation doctorate I, registration number DWD/6/0325/2022, request ID: dff09d10e905435f9d3d5a7171b8cca7. This work was also funded by the Smart Growth Operational Programme, project no. POIR.04.02.00-00-D003/20-00; European Funds, project no. RPWP.01.01.00-30-0004/18 and the Ministry of Science and Higher Education, project no. 21/529535/SPUB/SP/2022.

Data Availability Statement: The data presented in this study are available on request from the corresponding author.

Conflicts of Interest: The authors declare no conflicts of interest.

References

1. You, B.; Zhou, D.; Zhang, S.; Yang, F.; Ren, X. Preparation of Core–Shell Nanoparticle-based Hindered Amine Stabilizer and Its Application in Polyoxymethylene. *J. Appl. Polym. Sci.* **2012**, *126*, 1291–1299. [[CrossRef](#)]
2. Yang, J.; Fang, W.; Du, J.; Zhou, T. Investigation on the Mechanical, Thermal and Electrical Properties of Polyoxymethylene Composites Modified by Thermoplastic Polyurethane Elastomer and Carbon Fiber. *J. Thermoplast. Compos. Mater.* **2024**, *37*, 1135–1149. [[CrossRef](#)]
3. Tan, L.; Yang, J.; Li, C.; Zhang, G.; Ding, Q.; Sun, D.; Zhang, Y. Effect of Polyoxymethylene Fiber on the Mechanical Properties and Abrasion Resistance of Ultra-High-Performance Concrete. *Materials* **2023**, *16*, 7014. [[CrossRef](#)] [[PubMed](#)]

4. Zhang, L.; Zhuo, X.; Shi, H.; Yu, S.; Tian, H.; Chen, J.; Hao, Y.; Chen, L.; Liu, W.; Xie, Y. Effects of Glass Fiber Reinforcing and Thermal Post-treatment on the Mechanical Properties and Crystallization Behaviors of Polyoxymethylene. *J. Appl. Polym. Sci.* **2023**, *140*, 1–11. [[CrossRef](#)]
5. Heinlein, G.S.; Timpe, S.J. Development of Elastic and Plastic Properties of Polyoxymethylene during Bending Fatigue. *J. Appl. Polym. Sci.* **2014**, *131*, 40762. [[CrossRef](#)]
6. Tokarz, L.; Pawlowski, S.; Kedzierski, M. Polyoxymethylene Applications. In *Polyoxymethylene Handbook*; Wiley: Hoboken, NJ, USA, 2014; pp. 153–161.
7. Mohsenzadeh, R.; Majidi, H.; Soltanzadeh, M.; Shelesh-Nezhad, K. Wear and Failure of Polyoxymethylene/Calcium Carbonate Nanocomposite Gears. *Proc. Inst. Mech. Eng. Part J J. Eng. Tribol.* **2020**, *234*, 811–820. [[CrossRef](#)]
8. Galeja, M.; Wypiór, K.; Wachowicz, J.; Kędzierski, P.; Hejna, A.; Marć, M.; Klewicz, K.; Gabor, J.; Okła, H.; Swinarew, A.S. POM/EVA Blends with Future Utility in Fused Deposition Modeling. *Materials* **2020**, *13*, 2912. [[CrossRef](#)]
9. Yang, W.; Wang, X.; Yan, X.; Guo, Z. Toughened Polyoxymethylene by Polyolefin Elastomer and Glycidyl Methacrylate Grafted High-density Polyethylene. *Polym. Eng. Sci.* **2017**, *57*, 1119–1126. [[CrossRef](#)]
10. Mehrabzadeh, M.; Rezaie, D. Impact Modification of Polyacetal by Thermoplastic Elastomer Polyurethane. *J. Appl. Polym. Sci.* **2002**, *84*, 2573–2582. [[CrossRef](#)]
11. Pielichowski, K.; Leszczynska, A. Structure-Property Relationships in Polyoxymethylene/Thermoplastic Polyurethane Elastomer Blends. *J. Polym. Eng.* **2005**, *25*, 359–373. [[CrossRef](#)]
12. Uthaman, N.; Majeed, A. Impact Modification of Polyoxymethylene (POM). *e-Polymers* **2006**, *6*. [[CrossRef](#)]
13. Ren, X.; Chen, L.; Zhao, H.; Dan, Y.; Cai, X. Acrylate Elastomer Toughened and UV Stabilized Polyoxymethylene. *J. Macromol. Sci. Part B* **2007**, *46*, 411–421. [[CrossRef](#)]
14. Zhou, D.; You, B.; Wu, G.; Ren, X. Mechanical Properties and Surface Morphology of Photodegraded Polyoxymethylene Modified by a Core-Shell Acrylate Elastomer with UV Stabilization. *Polym. Int.* **2012**, *61*, 971–981. [[CrossRef](#)]
15. Liang, J.-Z.; He, L. Melt Flow Properties and Melt Density of POM/EVA/HDPE Nanocomposites. *Polym. Plast. Technol. Eng.* **2011**, *50*, 1338–1343. [[CrossRef](#)]
16. Liang, J.-Z.; Wang, F. Tensile Properties of Polyformaldehyde Blends and Nanocomposites. *J. Polym. Eng.* **2015**, *35*, 417–422. [[CrossRef](#)]
17. Liang, J.-Z. Melt Extrudate Swell Behavior of POM/EVA/HDPE/Nano-CaCO₃ Composites. *J. Polym. Eng.* **2013**, *33*, 19–26. [[CrossRef](#)]
18. Andrzejewski, J.; Skórczewska, K.; Kloziński, A. Improving the Toughness and Thermal Resistance of Polyoxymethylene/Poly(Lactic Acid) Blends: Evaluation of Structure-Properties Correlation for Reactive Processing. *Polymers* **2020**, *12*, 307. [[CrossRef](#)]
19. Kanai, H.; Sullivan, V.; Auerbach, A. Impact Modification of Engineering Thermoplastics. *J. Appl. Polym. Sci.* **1994**, *53*, 527–541. [[CrossRef](#)]
20. Mehta, I.K.; Kumar, S.; Chauhan, G.S.; Misra, B.N. Grafting onto Isotactic Polypropylene. III. Gamma Rays Induced Graft Copolymerization of Water Soluble Vinyl Monomers. *J. Appl. Polym. Sci.* **1990**, *41*, 1171–1180. [[CrossRef](#)]
21. Jang, G.; Cho, W.; Ha, C. Crystallization Behavior of Polypropylene with or without Sodium Benzoate as a Nucleating Agent. *J. Polym. Sci. B Polym. Phys.* **2001**, *39*, 1001–1016. [[CrossRef](#)]
22. Jiang, X.; Zhao, S.; Meng, X.; Xin, Z. Effect of the Metal Phenylphosphonates on the Nonisothermal Crystallization and Performance of Isotactic Polypropylene. *J. Polym. Sci. B Polym. Phys.* **2019**, *57*, 161–173. [[CrossRef](#)]
23. Meng, X.; Gong, W.; Chen, W.; Shi, Y.; Sheng, Y.; Zhu, S.; Xin, Z. Isothermal and Non-Isothermal Crystallization of Isotactic Polypropylene in the Presence of an α Nucleating Agent and Zeolite 13X. *Thermochim. Acta* **2018**, *667*, 9–18. [[CrossRef](#)]
24. Ningrum, D.; Soehardjono, A.; Suseno, H.; Wibowo, A. Analysis of the Effect of Using Covid-19 Medical Mask Waste with Polypropylene on the Compressive Strength and Split Tensile Strength of High-Performance Concrete. *East. Eur. J. Enterp. Technol.* **2023**, *1*, 40–46. [[CrossRef](#)]
25. Mubarak, Y.A.; Abu-Halimeh, R.; Schubert, D. Thermal and Morphological Properties of Polypropylene/Styrene-Butadiene-Styrene Nanocomposites. *Polym. Plast. Technol. Eng.* **2018**, *57*, 1542–1553. [[CrossRef](#)]
26. Natta, G.; Pino, P.; Corradini, P.; Danusso, F.; Mantica, E.; Mazzanti, G.; Moraglio, G. Crystalline High Polymers of α -Olefins. *J. Am. Chem. Soc.* **1955**, *77*, 1708–1710. [[CrossRef](#)]
27. Horikoshi, R.; Kobayashi, Y.; Kageyama, H. Illustrating Catalysis with Interlocking Building Blocks: Correlation between Structure of a Metallocene Catalyst and the Stereoregularity of Polypropylene. *J. Chem. Educ.* **2013**, *90*, 620–622. [[CrossRef](#)]
28. Harmon, R.E.; SriBala, G.; Broadbelt, L.J.; Burnham, A.K. Insight into Polyethylene and Polypropylene Pyrolysis: Global and Mechanistic Models. *Energy Fuels* **2021**, *35*, 6765–6775. [[CrossRef](#)]
29. Zhang, Y.; Xin, Z. Isothermal Crystallization Behaviors of Isotactic Polypropylene Nucleated with α/β Compounding Nucleating Agents. *J. Polym. Sci. B Polym. Phys.* **2007**, *45*, 590–596. [[CrossRef](#)]
30. Zhang, X.; Wang, X.; Dong, B.; Zheng, G.; Chen, J.; Shen, C.; Park, C.B. Synergetic Effect of Crystal Nucleating Agent and Melt Self-Enhancement of Isotactic Polypropylene on Its Rheological and Microcellular Foaming Properties. *J. Cell. Plast.* **2021**, *57*, 101–121. [[CrossRef](#)]
31. Malpass, D.B. *Introduction to Industrial Polyethylene*; Wiley: Hoboken, NJ, USA, 2010; ISBN 9780470625989.

32. Poulakis, J.G.; Varelidis, P.C.; Papaspyrides, C.D. Recycling of Polypropylene-Based Composites. *Adv. Polym. Technol.* **1997**, *16*, 313–322. [CrossRef]
33. Handayani, S.U.; Fahrudin, M.; Mangestiyono, W.; Hadi Muhamad, A.F. Mechanical Properties of Commercial Recycled Polypropylene from Plastic Waste. *J. Vocat. Stud. Appl. Res.* **2021**, *3*, 1–4. [CrossRef]
34. Azevedo, R.; Silveira, E.; Vieira, L.; Panzera, T.H.; Luis Christoforo, A.; Donizeti Varanda, L.; Antonio Rocco Lahr, F. Evaluation of the Temperature in the Painting Process on the Mechanical Properties of Polypropylene Used in Automotive Bumpers. *Int. J. Mater. Eng.* **2014**, *4*, 79–82. [CrossRef]
35. Cimmino, S.; Silvestre, C.; Duraccio, D.; Pezzuto, M. Effect of Hydrocarbon Resin on the Morphology and Mechanical Properties of Isotactic Polypropylene/Clay Composites. *J. Appl. Polym. Sci.* **2011**, *119*, 1135–1143. [CrossRef]
36. Kuznetsova, I.S.; Ryabchenkova, V.G.; Korniyushina, M.P.; Savrasov, I.P.; Vostrov, M.S. Polypropylene Fiber Is an Effective Way to Struggle with the Explosion-Like Destruction of Concrete in Case of Fire. *Stroit. Mater.* **2018**, *765*, 15–20. [CrossRef]
37. Darweesh, M.H.; El-Taweel, S.H.; Stoll, B. Miscibility and Rigid Amorphous Phase in Blends of Polypropylene with Poly(Propylene-co-ethylene). *J. Appl. Polym. Sci.* **2022**, *139*, e52711. [CrossRef]
38. Pradeep, S.A.; Iyer, R.K.; Kazan, H.; Pilla, S. Automotive Applications of Plastics: Past, Present, and Future. In *Applied Plastics Engineering Handbook*; Elsevier: Amsterdam, The Netherlands, 2017; pp. 651–673.
39. Maddah, H.A. Polypropylene as a Promising Plastic: A Review. *Am. J. Polym. Sci.* **2016**, *6*, 1–11. [CrossRef]
40. Yazdani, H.; Morshedjan, J.; Khonakdar, H.A. Effect of Maleated Polypropylene and Impact Modifiers on the Morphology and Mechanical Properties of PP/Mica Composites. *Polym. Compos.* **2006**, *27*, 614–620. [CrossRef]
41. Takubo, E.; Hiejima, Y.; Nishioka, K.; Nitta, K. Effects of Poly(Propylene Carbonate) Additive Prepared from Carbon Dioxide on the Tensile Properties of Polypropylene. *J. Appl. Polym. Sci.* **2017**, *134*, 45266. [CrossRef]
42. Karger-Kocsis, J.; Kalló, A.; Kuleznev, V.N. Phase Structure of Impact-Modified Polypropylene Blends. *Polymers* **1984**, *25*, 279–286. [CrossRef]
43. Murillo, E.A.; López, B.L. Study of the Impact Resistance of Physically and Dynamically Vulcanized Mixtures of PP/EPDM. *Macromol. Symp.* **2006**, *242*, 131–139. [CrossRef]
44. Guo, M.; Zhou, X.; Dai, G.; Hu, F. Polypropylene/Ethylene-Octene Copolymer/Organic-Montmorillonite Nanocomposites. *Polym. Polym. Compos.* **2005**, *13*, 173–180. [CrossRef]
45. Maciel, A.; Salas, V.; Manero, O. PP/EVA Blends: Mechanical Properties and Morphology. Effect of Compatibilizers on the Impact Behavior. *Adv. Polym. Technol.* **2005**, *24*, 241–252. [CrossRef]
46. Ma, Y.; Xin, C.; Huang, G.; Wang, Y.; He, Y. Fundamental Influences of Propylene-based Elastomer on the Foaming Properties of High Melt Strength Polypropylene Based on Extrusion Foaming. *Polym. Eng. Sci.* **2022**, *62*, 3973–3984. [CrossRef]
47. Yang, J.; Li, F.; Guan, C.; Xu, X.; Zhong, L.; Gao, Y.; Han, Y.; Yan, N.; Zhao, G.; Jiang, W. Brittle-Ductile Transition of Impact PP Blends: Effect of Modulus Ratio of PP Matrix to Impact Modifier. *Polym. Bull.* **2023**, *80*, 4459–4471. [CrossRef]
48. Shen, Y.; Tian, H.; Pan, W.; Feng, J.; Wang, D.; Ning, N.; Tian, M.; Zhang, L. Unexpected Improvement of Both Mechanical Strength and Elasticity of EPDM/PP Thermoplastic Vulcanizates by Introducing β -Nucleating Agents. *Macromolecules* **2021**, *54*, 2835–2843. [CrossRef]
49. Wang, X.; Han, X.; Xu, R. Versatile Propylene-Based Polyolefins with Tunable Molecular Structure through Tailor-Made Catalysts and Polymerization Process. In *Polypropylene—Polymerization and Characterization of Mechanical and Thermal Properties*; IntechOpen: London, UK, 2020.
50. Švab, I.; Musil, V.; Pustak, A.; Šmit, I. Wollastonite-reinforced Polypropylene Composites Modified with Novel Metallocene EPR Copolymers. II. Mechanical Properties and Adhesion. *Polym. Compos.* **2009**, *30*, 1091–1097. [CrossRef]
51. Delva, L.; De Tandt, E.; Ragaert, K. International Conference on Polymers and Moulds Innovations—PMI 2018. In *Combining Polymeric Waste Streams to Improve Functional Properties of Post-Consumer Mixed Polyolefines*; Institute of Polymers and Composites, University of Minho: Minho, Portugal, 2018.
52. White Paper: Performance Comparison between Polypropylene-Vistamaxx Polymer Blends Made from Dry-Blend and from Melt-Blend, ExxonMobil Technology and Engineering, Product Solutions Technology. Available online: <https://international.exxonmobilchemical.com/en/library/library-detail?assetid=104603> (accessed on 18 September 2024).
53. Vuluga, Z.; Corobea, M.; Elizetxea, C.; Ordonez, M.; Ghiurea, M.; Raditoiu, V.; Nicolae, C.; Florea, D.; Iorga, M.; Somoghi, R.; et al. Morphological and Tribological Properties of PMMA/Halloysite Nanocomposites. *Polymers* **2018**, *10*, 816. [CrossRef]
54. Ali, U.; Karim, K.J.B.A.; Buang, N.A. A Review of the Properties and Applications of Poly (Methyl Methacrylate) (PMMA). *Polym. Rev.* **2015**, *55*, 678–705. [CrossRef]
55. An, J.; Kang, B.-H.; Choi, B.-H.; Kim, H.-J. Observation and Evaluation of Scratch Characteristics of Injection-Molded Poly(Methyl Methacrylate) Toughened by Acrylic Rubbers. *Tribol. Int.* **2014**, *77*, 32–42. [CrossRef]
56. Pawar, E. A Review Article on Acrylic PMMA. *IOSR J. Mech. Civ. Eng.* **2016**, *13*, 1–4.
57. Godiya, C.B.; Gabrielli, S.; Materazzi, S.; Pianesi, M.S.; Stefanini, N.; Marcantoni, E. Depolymerization of Waste Poly(Methyl Methacrylate) Scraps and Purification of Depolymerized Products. *J. Environ. Manag.* **2019**, *231*, 1012–1020. [CrossRef] [PubMed]
58. Nampoothiri, P.K.; Gandhi, M.N.; Kulkarni, A.R. Elucidating the Stabilizing Effect of Oleic Acid Coated LaF₃: Nd³⁺ Nanoparticle Surface in the Thermal Degradation of PMMA Nanocomposites. *Mater. Chem. Phys.* **2017**, *190*, 45–52. [CrossRef]

59. Tomić, N.Z.; Marinković, A.D.; Veljović, Đ.; Trifković, K.; Lević, S.; Radojević, V.; Jančić Heinemann, R. A New Approach to Compatibilization Study of EVA/PMMA Polymer Blend Used as an Optical Fibers Adhesive: Mechanical, Morphological and Thermal Properties. *Int. J. Adhes. Adhes.* **2018**, *81*, 11–20. [CrossRef]
60. Poomalai, P. Siddaramaiah Studies on Poly(Methyl Methacrylate) (PMMA) and Thermoplastic Polyurethane (TPU) Blends. *J. Macromol. Sci. Part A* **2005**, *42*, 1399–1407. [CrossRef]
61. Mina, M.F.; Ania, F.; Baltá Calleja, F.J.; Asano, T. Microhardness Studies of PMMA/Natural Rubber Blends. *J. Appl. Polym. Sci.* **2004**, *91*, 205–210. [CrossRef]
62. Chen, Y.; Wang, W.; Yuan, D.; Xu, C.; Cao, L.; Liang, X. Bio-Based PLA/NR-PMMA/NR Ternary Thermoplastic Vulcanizates with Balanced Stiffness and Toughness: “Soft–Hard” Core–Shell Continuous Rubber Phase, In Situ Compatibilization, and Properties. *ACS Sustain. Chem. Eng.* **2018**, *6*, 6488–6496. [CrossRef]
63. Rahman, S.S.; Mahmud, M.B.; Monfared, A.R.; Lee, P.C.; Park, C.B. Achieving Outstanding Toughness of PMMA While Retaining Its Strength, Stiffness, and Transparency Using in Situ Developed TPEE Nanofibrils. *Compos. Sci. Technol.* **2023**, *236*, 109994. [CrossRef]
64. KURARITY™ Acrylic Block Copolymer Technical Information. Available online: <https://www.elastomer.kuraray.com/wp-content/uploads/2021/04/Kuraray-Elastomer-Product-Brochures-Kurarity-Technical-Information.pdf> (accessed on 8 May 2024).
65. Lu, W.; Hong, K.; Mays, J. New Class of Thermoplastic Elastomers Based on Acrylic Block Copolymers. *Adv. Thermoplast. Elastomers Chall. Oppor.* **2024**, 125–149. [CrossRef]
66. Lu, W.; Goodwin, A.; Wang, Y.; Yin, P.; Wang, W.; Zhu, J.; Wu, T.; Lu, X.; Hu, B.; Hong, K.; et al. All-Acrylic Superelastomers: Facile Synthesis and Exceptional Mechanical Behavior. *Polym. Chem.* **2018**, *9*, 160–168. [CrossRef]
67. Uchiumi, N.; Hamada, K.; Kato, M.; Ono, T.; Yaginuma, S.; Ishiura, K. Preparation Process of Acrylic Acid Ester Polymer. US6329480B1, 15 December 1999.
68. Hamada, K.; Ishiura, K.; Kato, M.; Yaginuma, S. Anionic Polymerization Process, and Process for Producing a Polymer by the Anionic Polymerization Process. EP1078942A1, 23 August 2000.
69. Hadjichristidis, N.; Hirao, A. (Eds.) *Anionic Polymerization*; Springer: Tokyo, Japan, 2015; ISBN 978-4-431-54185-1.
70. ISO 20753:2019-01; Plastics—Test specimens. ISO: Geneva, Switzerland, 2019.
71. ISO 19403-2:2017; Paints and varnishes—Wettability. ISO: Geneva, Switzerland, 2017.
72. ISO 1133-1:2022; Plastics—Determination of the melt mass-flow rate (MFR) and melt volume-flow rate (MVR) of thermoplastics. ISO: Geneva, Switzerland, 2022.
73. ISO 527-1:2019; Plastics—Determination of Tensile Properties. ISO: Geneva, Switzerland, 2019.
74. ISO 179-1:2010; Plastics—Determination of Charpy Impact Properties. ISO: Geneva, Switzerland, 2010.
75. ISO 11357-1:2023; Plastics—Differential scanning calorimetry (DSC). ISO: Geneva, Switzerland, 2023.
76. Turner, B.N.; Strong, R.; Gold, S.A. A Review of Melt Extrusion Additive Manufacturing Processes: I. Process Design and Modeling. *Rapid Prototyp. J.* **2014**, *20*, 192–204. [CrossRef]
77. Shenoy, A.V.; Saini, D.R. Melt Flow Index: More than Just a Quality Control Rheological Parameter. Part I. *Adv. Polym. Technol.* **1986**, *6*, 1–58. [CrossRef]
78. Shenoy, A.V.; Saini, D.R.; Nadkarni, V.M. Melt Rheology of Polymer Blends from Melt Flow Index. *Int. J. Polym. Mater. Polym. Biomater.* **1984**, *10*, 213–235. [CrossRef]
79. Hel, C.L.; Bounor-Legaré, V.; Catherin, M.; Lucas, A.; Thèvenon, A.; Cassagnau, P. TPV: A New Insight on the Rubber Morphology and Mechanic/Elastic Properties. *Polymers* **2020**, *12*, 2315. [CrossRef] [PubMed]
80. Machado, A.V.; Antunes, C.F.; van Duin, M.; Zatloukal, M. *Phase Inversion of EPDM/PP Blends: Effect of Viscosity Ratio*; American Institute of Physics: College Park, MD, USA, 2011; pp. 240–247.
81. Poomalai, P.; Ramaraj, B. Siddaramaiah Poly(Methyl Methacrylate) Toughened by Ethylene-vinyl Acetate Copolymer: Physico-mechanical, Thermal, and Chemical Properties. *J. Appl. Polym. Sci.* **2007**, *104*, 3145–3150. [CrossRef]
82. Sang, X.M.; Zhang, L.; Wang, R.Z.; Chen, X.G.; An, M.; Shen, Y. Study on Preparation and Properties of Polystyrene/Styrene-Ethylene/Butylene-Styrene Composites. *Adv. Mater. Res.* **2011**, 284–286, 1886–1889. [CrossRef]
83. Kumbhani, K.J.; Kent, E.G. *Improving Polyolefin Properties with Butyl*; SAE Technical Paper 811348; SAE International: Warrendale, PA, USA, 1981.
84. Ucar, I.O.; Doganci, M.D.; Cansoy, C.E.; Erbil, H.Y.; Avramova, I.; Suzer, S. Combined XPS and contact angle studies of ethylene vinyl acetate and polyvinyl acetate blends. *Appl. Surf. Sci.* **2011**, *257*, 9587–9594. [CrossRef]
85. Sobczak, R.; Nitkiewicz, Z.; Koszkuł, J. Struktura Nadcząsteczkowa i Własności Termiczne Kompozytów Na Osnowie Polipropylenu Wzmocnianych Włóknem Szklanym. *Kompozyty* **2003**, *3*, 343–348.
86. Pielichowski, K.; Leszczyńska, A. Polyoxymethylene-Based Nanocomposites with Montmorillonite: An Introductory Study. *Polimery* **2022**, *51*, 143–149. [CrossRef]

Disclaimer/Publisher’s Note: The statements, opinions and data contained in all publications are solely those of the individual author(s) and contributor(s) and not of MDPI and/or the editor(s). MDPI and/or the editor(s) disclaim responsibility for any injury to people or property resulting from any ideas, methods, instructions or products referred to in the content.